Int J Legal Med (2016) 130:163–172
DOI 10.1007/s00414-015-1251-x

ORIGINAL ARTICLE

Detection of satellite cells during skeletal muscle wound healing in rats: time-dependent expressions of Pax7 and MyoD in relation to wound age

Zhi-Ling Tian[1] · Shu-Kun Jiang[1] · Miao Zhang[1] · Meng Wang[1] · Jiao-Yong Li[1] · Rui Zhao[1] · Lin-Lin Wang[1] · Shan-Shan Li[1] · Min Liu[1] · Meng-Zhou Zhang[1] · Da-Wei Guan[1]

Received: 19 May 2015 / Accepted: 12 August 2015 / Published online: 27 August 2015

Abstract The study was focused on time-dependent expressions of paired-box transcription factor 7 (Pax7) and myoblast determination protein (MyoD) during skeletal muscle wound healing. An animal model of skeletal muscle contusion was established in 40 Sprague–Dawley male rats. Samples were taken at 1, 3, 5, 7, 9, 13, 17, and 21 days after injury, respectively (five rats in each posttraumatic interval). Five rats were employed as control. By morphometric analysis, the data based on the number of $Pax7^+/MyoD^-$, $Pax7^+/MyoD^+$, and $Pax7^-/MyoD^+$ cells were highly correlated with the wound age. Pax7 and MyoD expressions were upregulated after injury by Western blot and quantitative real-time PCR assays. The relative quantity of Pax7 protein peaked at 5 days after injury, which was >1.13, and decreased thereafter. Similarly, the relative quantity of MyoD mRNA expression peaked at 3 days after injury, which was >2.59. The relative quantity of Pax7 protein >0.73 or mRNA expression >2.38 or the relative quantity of MyoD protein >1.33 suggested a wound age of 3 to 7 days. The relative quantity of MyoD mRNA expression >2.02 suggested a wound age of 1 to 7 days post-injury. In conclusion, the expressions of Pax7 and MyoD are upregulated in a time-dependent manner during skeletal muscle wound healing, suggesting that Pax7 and MyoD may be potential markers for wound age estimation in skeletal muscle.

Keywords Wound age estimation · Skeletal muscle contusion · Satellite cell · Pax7 · MyoD

Introduction

Satellite cells are essential for muscle regeneration which is the key event in muscle healing [1, 2]. Upon muscle injury, satellite cells are activated, driven out of their quiescent states, and start to proliferate. Proliferating satellite cells, termed myogenic precursor cells or myoblasts, then stop their proliferation, undergo differentiation into myocytes, and fuse either with each other or damaged myofibers to repair injured muscle [3, 4]. While forming myotubes, a portion of satellite cells self-renew and eventually return to a quiescent state as satellite cells to respond to the next round of muscle injury and repair [5, 6]. Accumulated evidence demonstrates that the paired-box transcription factor 7 (Pax7) is a well-established marker for satellite cells in both the quiescent and activated states [2, 7–10], and its expression is sharply downregulated before differentiation [7]. Myoblast determination protein (MyoD) is expressed early in myogenesis to initiate proliferation of satellite cells and marks the proliferated and differentiated satellite cells [2, 8]. The interactions of Pax7 and MyoD determine satellite cell fate and contribute to maintaining the balance between satellite cell differentiation and self-renewal, which is required for muscle homeostasis [9]. Pax7 and MyoD specify the myogenic status of satellite cells as quiescent ($Pax7^+/MyoD^-$), activated/proliferating myoblasts ($Pax7^+/MyoD^+$), or differentiated ($Pax7^-/MyoD^+$) followed by cell fusion to form generated multinucleated myotubes [2, 7–10].

Electronic supplementary material The online version of this article (doi:10.1007/s00414-015-1251-x) contains supplementary material, which is available to authorized users.

✉ Da-Wei Guan
dwguan@aliyun.com; dwguan@mail.cmu.edu.cn

[1] Department of Forensic Pathology, China Medical University School of Forensic Medicine, No.77, Puhe Road, Shenbei New Area, Shenyang 110122, Liaoning Province, People's Republic of China

We speculated that dynamic expressions of Pax7 and MyoD may be closely related to wound age.

Wound age estimation is one of the most important tasks in the forensic practice [11–14], and most of the studies in the field are conducted using skin specimens in mice and human [14–20]. Only a few studies are reported on wound age estimation in skeletal muscles in which the markers cover the cannabinoid CB_2 receptor [21], troponin I [22], and α7 nicotine acetylcholine receptor [23]. In the present study, we investigated the dynamic expressions of Pax7 and MyoD to provide preliminary insight to wound age estimation in skeletal muscles.

Materials and methods

Animal model of skeletal muscle contusion

All animal protocols were conformed to the "Principles of Laboratory Animal Care" (National Institutes of Health publication no. 85-23, revised 1985) that sought to minimize both the number of animals used in a procedure and any suffering that they might experience and were performed according to the Guidelines for the Care and Use of Laboratory Animals of China Medical University. A reproducible muscle contusion model in rats was described previously [21, 24, 25]. Briefly, adult Sprague–Dawley male rats, weighing 300–320 g, were anesthetized by intraperitoneal injection with 2 % sodium pentobarbital (30 mg/kg). The right hindlimb was positioned on a board in a prone position by extending the knee and dorsiflexing the ankle to 90°. A single impact at velocity of 3 m/s was delivered to the gastrocnemius and soleus of the right posterior limb. The size of impact interface of the counterpoise (weighing 500 g) was 1.127 cm^2. After injury, each rat was housed individually and kept under a 12-h light–dark cycle. The rats were fed with commercial rat chow and water ad libitum. All rats were killed by intraperitoneal injection of a lethal dose of pentobarbital (350 mg/kg) at 1, 3, 5, 7, 9, 13, 17, and 21 days post-trauma (five rats at each posttraumatic interval). Gastrocnemius was taken and equally divided into two blocks. One block was used for morphological evaluation, and another was used for molecular biological assays. For the five control rats, gastrocnemius was harvested after anesthetization with an overdose of pentobarbital. No bone fracture was detected at dissection.

Tissue preparation and immunofluorescence microscopy

The skeletal muscle specimens were fixed in 4 % paraformaldehyde in phosphate-buffered saline (pH 7.4) and embedded in paraffin, followed by being sectioned at a thickness of 5 μm. The dynamic distribution of satellite cells in different myogenic status with extension of wound age was detected by localization of Pax7 and MyoD. Briefly, deparaffinized sections were blocked with 5 % normal donkey serum (Jackson ImmunoResearch, PA, USA). Then, the sections were incubated with rabbit anti-Pax7 polyclonal antibody (pAb) (dilution 1:100; sc-25409, Santa Cruz Biotechnology, CA, USA) and mouse anti-MyoD monoclonal antibody (mAb) (dilution 1:50; sc-71629, Santa Cruz Biotechnology, CA, USA) overnight at 4 °C. Thereafter, the sections were incubated with Alexa Fluor® 488 donkey anti-rabbit IgG (dilution 1:200; A21206, Invitrogen, CA, USA) and Alexa Fluor® 594 donkey anti-mouse IgG (dilution 1:200; A21203, Invitrogen, CA, USA) at room temperature (RT) for 2 h; the nuclei were counterstained with Hoechst 33258. Normal rabbit or mouse IgG was used instead of primary antibodies as negative control. The sections were mounted and observed under a fluorescence microscope. The immunofluorescent images were digitally merged. In addition, hematoxylin–eosin (H-E) staining was conventionally conducted.

For positive cell number evaluation, ten microscopic fields were randomly selected at 400-fold magnification in the contused zone in each section, and the number of $Pax7^+/MyoD^-$, $Pax7^+/MyoD^+$, or $Pax7^-/MyoD^+$ cells was calculated in each microscopic field. The average number of the ten selected microscopic fields was evaluated in each wound specimen. All measurements and data analysis were performed independently by two pathologists.

Protein preparation and immunoblotting assay

The skeletal muscle samples were ground into powder with liquid nitrogen using a grinder and homogenized with a sonicator in RIPA buffer (sc-24948, Santa Cruz Biotechnology, CA, USA) containing protease inhibitors at 4 °C. Homogenates were centrifuged at 12,000×*g* for 30 min three times at 4 °C, and the resulting supernatants were collected. The protein concentrations were determined using the bicinchoninic acid method. Aliquots of the supernatants were diluted in an equal volume of 6× electrophoresis sample buffer and boiled for 5 min. Protein lysates (30 μg) were separated on a 12 % sodium dodecyl sulfate-poly-acrylamide electrophoresis gel and transferred onto polyvinylidene fluoride membranes (Millipore, Billerica, MA, USA). After being blocked with 5 % non-fat dry milk in Tris-buffered saline-Tween-20 at RT for 2 h, the membranes were incubated respectively with rabbit anti-Pax7 pAb (dilution 1:200; sc-25409, Santa Cruz Biotechnology, CA, USA) and mouse anti-MyoD mAb (dilution 1:200; sc-71629, Santa Cruz Biotechnology, CA, USA) at 4 °C overnight. Then, the membranes were incubated with horseradish peroxidase-conjugated secondary antibody at RT for 2 h. The blotting

was visualized with Western blotting luminol reagent (sc-2048, Santa Cruz Biotechnology, CA, USA) and by the Electrophoresis Gel Imaging Analysis System (MF-ChemiBIS 3.2, DNR Bio-Imaging Systems, ISR). Subsequently, densitometric analyses of the bands were semi-quantitatively conducted using Scion Image software (Scion Corporation, MD, USA). The relative protein levels were calculated by comparison with the amount of glyceraldehyde 3-phosphate dehydrogenase (GAPDH) (#G13-61M, SignalChem, Canada) as a loading control.

Total RNA extraction and quantitative real-time PCR

Total RNA was isolated from the skeletal muscle specimens with RNAiso Plus (9108, Takara Biotechnology, Shiga, Japan) according to the manufacturer's instructions. OD values of each RNA sample were measured by ultraviolet spectrophotometer. A260/A280 ranged from 1.8 to 2.0. Then, the RNA was reverse-transcribed into cDNA using the PrimeScript™ RT reagent Kit (RR037A, Takara Biotechnology, Shiga, Japan). cDNA synthesis was performed in a 20-μl reaction mixture. The resulting cDNA was used for quantitative real-time PCR (qPCR) with the sequence-specific primer pairs for *Pax7*, *Myod1*, and *Gapdh* (Table 1). qPCR amplification was performed by Applied Biosystems 7500 Real-Time PCR System using SYBR® PrimeScript™ RT-PCR Kit (RR081A, Takara Biotechnology, Shiga, Japan). To exclude any potential contamination, negative controls were also performed with dH_2O instead of cDNA during each run. No amplification product was detected. The qPCR procedure was repeated at least three times for each sample.

Statistical analysis

Data were expressed as mean±standard deviation (SD) and analyzed using PRISM 6.0 software. The one-way ANOVA was used for data analysis between two groups. Difference associated with $p<0.05$ was considered as statistically significant.

Results

Histological examination

In sections stained with H-E, hemorrhage, edema, and degeneration were observed in the contused skeletal muscles. A large number of polymorphonulcear cells (PMNs) appeared in wound zones at 1 day post-wounding (Fig. 1b). Round-shaped mononuclear cells (MNCs) appeared in wound zones at 1 day, which remarkably increased in number at 3 days post-wounding (Fig. 1c). At 3 days post-wounding, spindle-shaped fibroblastic cells (FBCs) appeared in the wound zones (Fig. 1c). From 5 to 9 days post-wounding, a large number of FBCs, concomitant with regenerated multinucleated myotubes, were observed in the wounds (Fig. 1d, e). From 13 to 21 days post-wounding, the nuclei of myotubes were gradually marginated, and some FBCs were still detectable in fibrotic tissue (Fig. 1f, g).

Double direct immunofluorescence for Pax7 and MyoD

To identify different myogenic status of satellite cells, co-localization of Pax7 and MyoD was conducted. Pax7 and MyoD were both detected in the nucleus (Fig. 2).

Morphometrically, total satellite cells (the sum of $Pax7^+/MyoD^-$, $Pax7^+/MyoD^+$, and $Pax7^-/MyoD^+$ cells) increased prominently from 3 days, peaked at 5 days after injury, and decreased thereafter. The number of satellite cells was >60 from 3 to 9 days ($p=0.035$) and >89 at 5 days ($p=0.012$) after injury (Fig. 3a). The number of $Pax7^+/MyoD^-$ cells increased significantly at 5 days post-injury, which was >6 ($p=0.018$) (Fig. 3b). $Pax7^+/MyoD^+$ cells increased from 3 days, peaked at 5 days after injury, and decreased thereafter. The number of $Pax7^+/MyoD^+$ cells was >16 from 5 to 7 days ($p=0.032$) and >34 at 5 days ($p=0.002$) after injury (Fig. 3c). $Pax7^-/MyoD^+$ cell number was >47 from 3 to 9 days ($p=0.023$) post-injury, which was significantly more than that at other posttraumatic intervals (Fig. 3d). The ratio of $Pax7^+/MyoD^-$ cells to total satellite cell number at 1 day post-injury (>0.29; $p<0.001$)

Table 1 Real-time PCR primer sequences

Gene	GenBank accession	Primer	Product size (bp)
Pax7	NM_001191984.1	Forward: 5′-GAT TAG CCG AGT GCT CAG AAT CAA G-3′ Reverse: 5′-GTC GGG TTC TGA TTC CAC GTC-3′	166
Myod1	NM_176079.1	Forward: 5′-GAC CCA GAA CTG GGA CAT GGA-3′ Reverse: 5′-TGA GTC GAA ACA CGG ATC ATC ATA G-3′	127
Gapdh	NM_017008.4	Forward: 5′-GGC ACA GTC AAG GCT GAG AAT G-3′ Reverse: 5′-ATG GTG GTG AAG ACG CCA GTA-3′	143

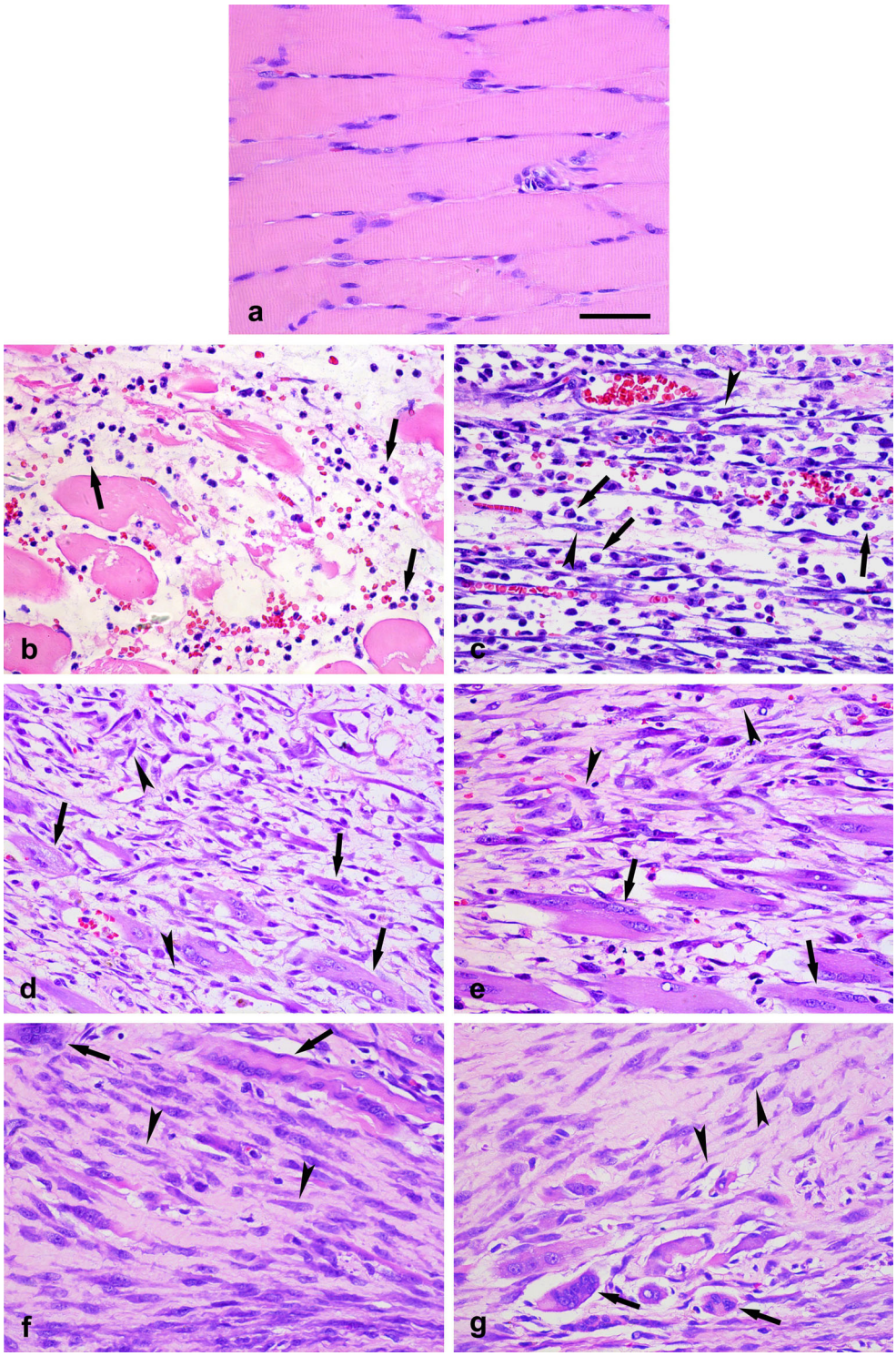

Fig. 1 H-E staining in rat skeletal muscle samples. **a** Normal skeletal muscles as a control. **b** PMNs are detected at 1 day after contusion (*arrows*). **c** Round-shaped MNCs (*arrows*) and spindle-shaped FBCs (*arrowheads*) are present in the injured tissue at 3 days after contusion. **d**, **e** FBCs (*arrowheads*), concomitant with regenerated multinucleated myotubes (*arrows*), are observed in the areas of contusion at 5 and 7 days after contusion. **f**, **g** The nuclei of myotubes are seen at subsarcolemmal position (*arrows*). Spindle-shaped FBCs (*arrowheads*) and fibrotic tissue are detected in the center of the wound zones at 13 and 21 days after injury. *Scale bar* 50 μm

showed a significant rise (Fig. 3e). The ratio of $Pax7^+/MyoD^+$ cells to total satellite cell number at 1 or 5 days post-injury (>0.51; $p=0.037$) was higher significantly than other posttraumatic intervals (Fig. 3f). The ratio of $Pax7^-/MyoD^+$ cells to total satellite cell number from 3 to 21 days post-injury was higher significantly than that at 1 day (<0.25; $p=0.021$) post-injury (Fig. 3g). The ratio of $Pax7^-/MyoD^+$ to $Pax7^+/MyoD^-$ cell number maintained a higher level which was >18.30 from 3 to 9 days ($p=0.046$) post-injury (Fig. 3h).

$Pax7^+$ cells ($Pax7^+/MyoD^+$ and $Pax7^+/MyoD^-$ cells) increased in number from 3 days and peaked at 5 days after

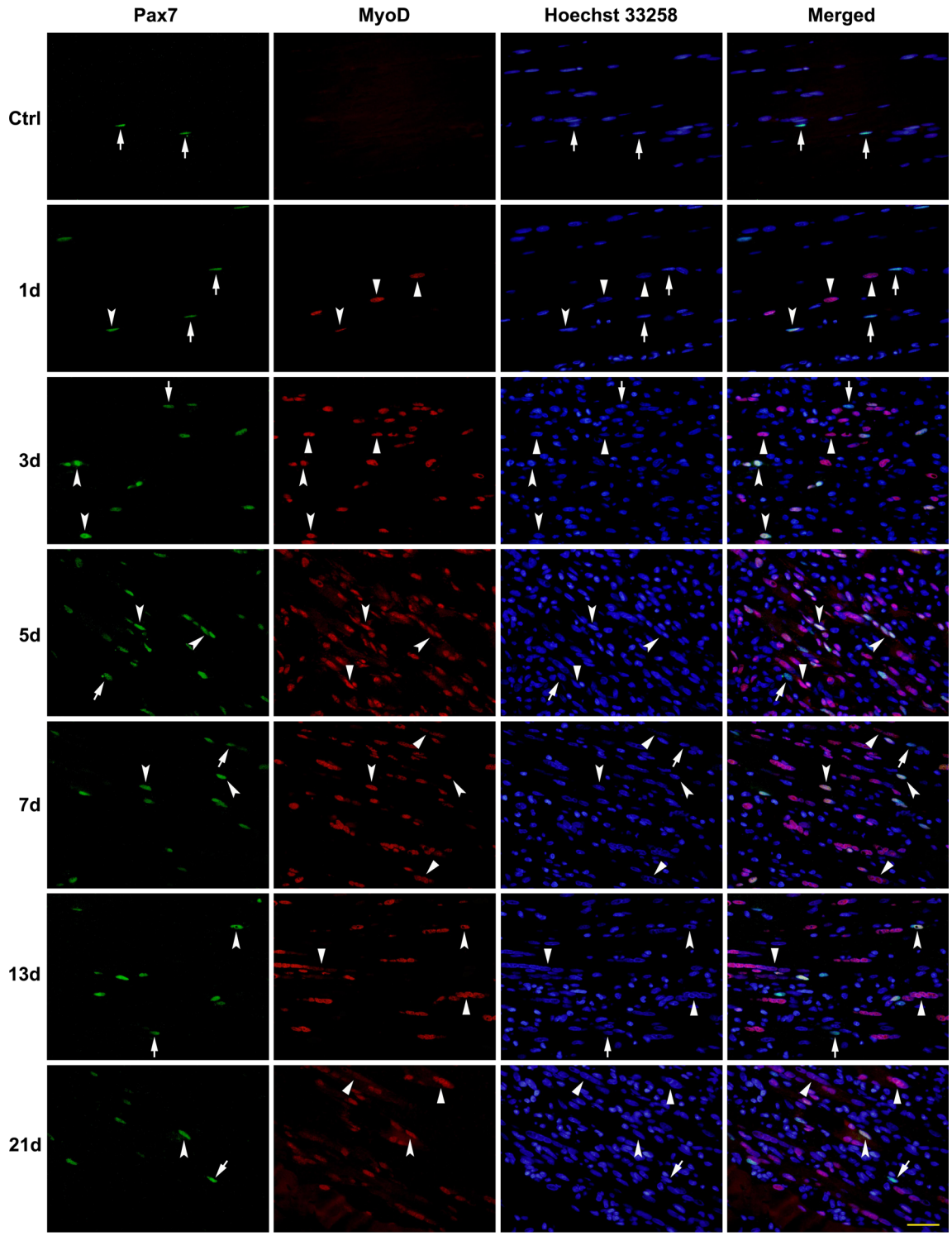

Fig. 2 Double immunofluorescent staining for identifying the satellite cells in different myogenic status. The sample was immunostained with anti-Pax7 (*green*) and anti-MyoD (*red*). Nuclei were counterstained with Hoechst 33258 (*blue*). The $Pax7^{+}/MyoD^{-}$ cells show cyan signals (*arrows*), $Pax7^{+}/MyoD^{+}$ cell bluish white signals (*arrowheads*), and $Pax7^{-}/MyoD^{+}$ cells pink signals (*triangles*) in the merged images. Representative results from at least three individual experiments are shown here. *Scale bar*, 50 μm

injury. The number of $Pax7^{+}$ cells was >20 from 5 to 7 days (p=0.023) and >39 at 5 days (p<0.001) after injury (Fig. 4a). $MyoD^{+}$ cells ($Pax7^{+}/MyoD^{+}$ and $Pax7^{-}/MyoD^{+}$ cells) increased significantly in number from 3 days, peaked at 5 days after injury, and decreased gradually with extension of posttraumatic

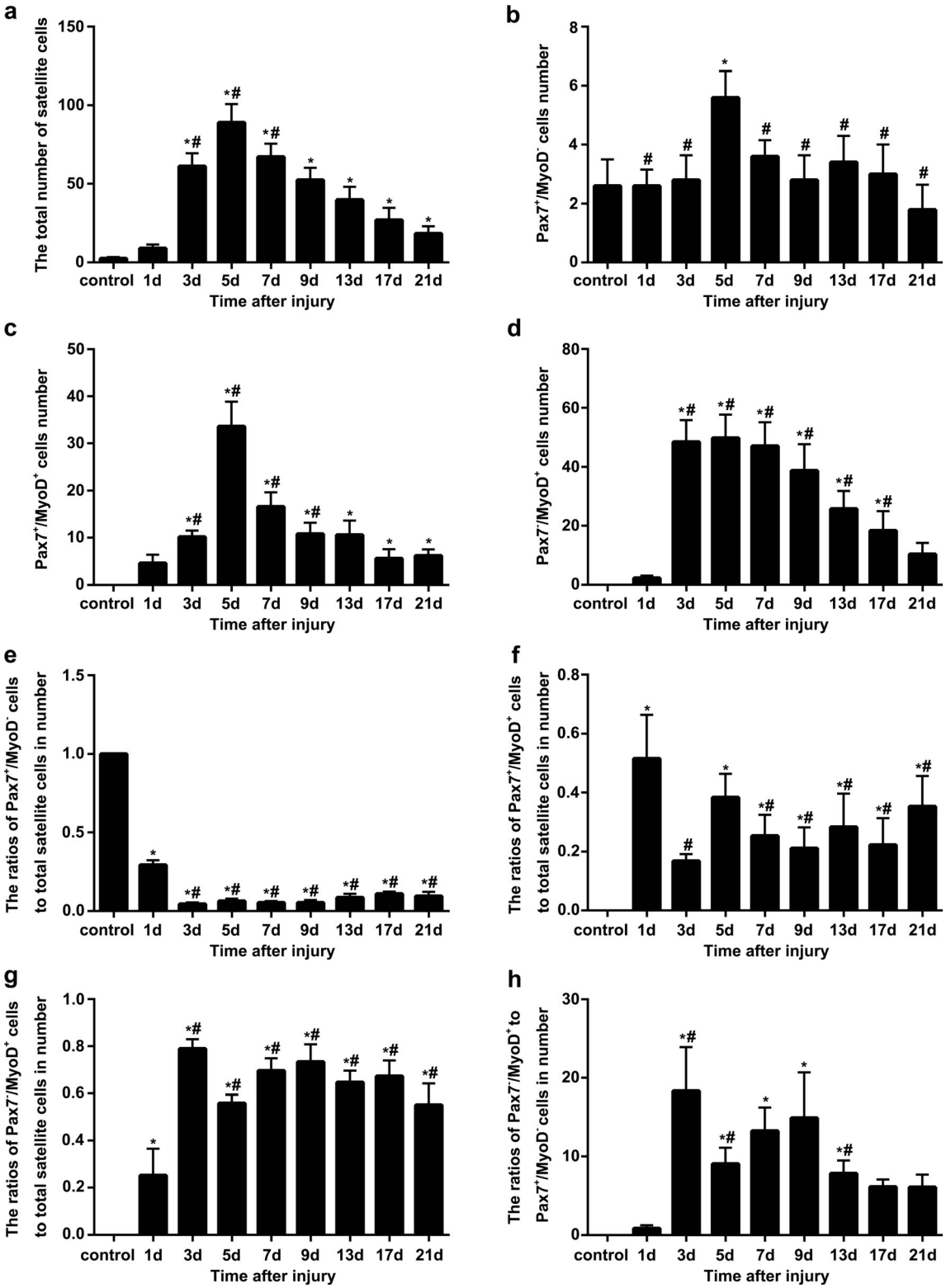

intervals. The number of $MyoD^+$ cells was >58 from 3 to 9 days (p=0.006) and >83 at 5 days (p=0.01) after injury (Fig. 4b). The ratio of $MyoD^+$ to $Pax7^+$ cells was >4.76 at 3 days post-injury, which was statistically significant as compared with other posttraumatic intervals except that at 9 days post-injury (p=0.027) (Fig. 4c).

The cell numbers and ratios in relation to wound age are summarized in Table 2.

◀ **Fig. 3** **a** The total number of satellite cells in relation to wound age. The total number of satellite cells peaked at 5 days post-wounding. **b** The average number of $Pax7^+/MyoD^-$ cells in relation to wound age. The average number of $Pax7^+/MyoD^-$ cells peaked at 5 days post-wounding. **c** The average number of $Pax7^+/MyoD^+$ cells in relation to wound age. The average number of $Pax7^+/MyoD^+$ cells peaked at 5 days post-wounding. **d** The average number of $Pax7^-/MyoD^+$ cells in relation to wound age. **e** The average ratios of $Pax7^+/MyoD^-$ cells to total satellite cells in number in relation to wound age. **f** The average ratios of $Pax7^+/MyoD^+$ cells to total satellite cells in number in relation to wound age. **g** The average ratios of $Pax7^-/MyoD^+$ cells to total satellite cells in number in relation to wound age. **h** The average ratios of $Pax7^-/MyoD^+$ cells to $Pax7^+/MyoD^-$ cells in number in relation to wound age. All data were presented as mean±SD and analyzed using one-way ANOVA. **a**, **c**, **h** $*p<0.05$ (vs control group); $^{\#}p<0.05$ (vs preceding posttraumatic group). **b** $*p<0.05$ (vs control group); $^{\#}p<0.05$ (vs 5 days group post-injury). **d**–**g**: $*p<0.05$ (vs control group); $^{\#}p<0.05$ (vs 1 day group post-injury)

Western blotting and qPCR

The expressions of Pax7 and MyoD protein were detected in all skeletal muscle specimens including the control by Western blotting (Fig. 5a, b). Both Pax7 and MyoD expressions were increased from 1 day post-injury. The relative quantity of Pax7 protein peaked at 5 days post-injury (>1.13; $p=0.013$) and decreased thereafter. The relative quantity of MyoD protein was >1.33 from 3 to 7 days ($p=0.025$) post-injury, which was significantly higher than that of the other posttraumatic interval. Significant difference in the relative expression levels of Pax7 and MyoD protein was respectively noted from 1 to 17 days and from 3 to 17 days post-wounding, as compared with that of control ($p<0.001$; Fig. 5c, d). And significant differences in the relative intensity of Pax7 and MyoD to GAPDH were respectively observed between 3, 5, 7, and 9 days injury groups and their preceding groups ($p<0.05$; Fig. 5c) and between 3 and 9 days injury groups and their preceding groups ($p<0.05$; Fig. 5d).

Relative quantities of Pax7 and MyoD mRNA expressions were assayed by qPCR throughout the 21 days after contusion. Similar to the results of Western blotting, the levels of Pax7 and MyoD mRNA were upregulated after injury. The relative quantity of Pax7 mRNA expression was >2.38 from 3 to 7 days ($p<0.001$) post-injury, which was significantly higher than that of the other posttraumatic intervals. The relative quantity of MyoD mRNA expression reached the peak at 3 days after injury, which was >2.59 ($p=0.018$). Significant difference in the relative quantities of Pax7 and MyoD mRNA expression was observed respectively from 3 to 9 days ($p<0.05$) and from 1 to 7 days ($p<0.001$) post-wounding, as compared with that of control (Fig. 6a, b). Significant differences in the relative quantities of Pax7 and MyoD mRNA expression were respectively observed between 3 and 9 days injury group and their preceding groups ($p<0.001$; Fig. 6a) and between 3, 5, and 9 days injury groups and their preceding groups ($p<0.05$; Fig. 6b).

The assays of Pax7 and MyoD by Western blot and qPCR in relation to wound age are summarized in Table 2.

Discussion

In response to muscle injury, quiescent satellite cells become activated and migrate to the injured site. The activated satellite cells are responsible for muscle regeneration, and a small proportion of activated satellite cells are back to quiescence to sustain the satellite cells pool [26]. Pax7 and MyoD are essential for muscle regeneration. Pax7 maintains satellite cell proliferation and prevents early myogenic differentiation and apoptotic cell death. Pax7 gene abrogation reduces satellite cells significantly, resulting in the failure of muscle growth and regeneration [8]. Pax7 regulates MyoD expression by binding directly proximal promoters of MyoD [27]. MyoD is closely involved in satellite cell activation, proliferation, and differentiation during muscle development and regeneration [28]. Satellite cells fail to differentiate and fuse in MyoD knockout animals, which leads to severely impaired muscle regeneration [29]. The activated satellite cells downregulate Pax7 expression and upregulate MyoD expression simultaneously in vitro [9]. In the present study, however, Pax7 and MyoD were significantly upregulated simultaneously after skeletal

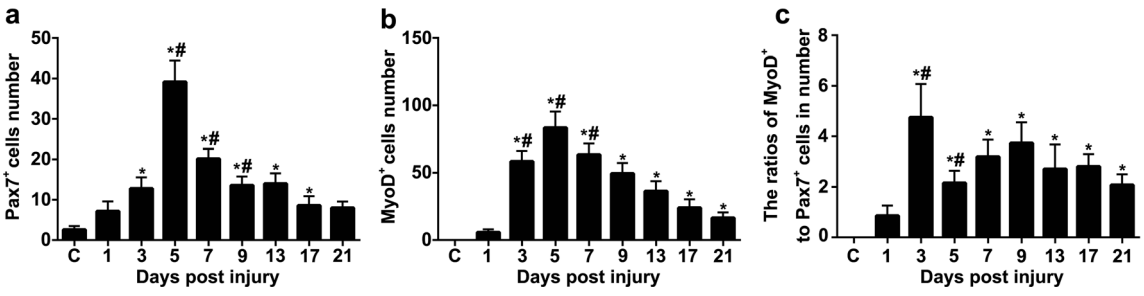

Fig. 4 **a** The average number of $Pax7^+$ cells in relation to wound age. The average number of $Pax7^+$ cells peaked at 5 days post-wounding. **b** The average number of $MyoD^+$ cells in relation to wound age. The average number of $MyoD^+$ cells peaked at 5 days post-wounding. **c** The average ratios of $MyoD^+$ to $Pax7^+$ cells in number in relation to wound age. All data were presented as mean±SD and analyzed using one-way ANOVA. $*p<0.05$ (vs control group); $^{\#}p<0.05$ (vs preceding posttraumatic group)

Table 2 Results in relation to wound age

Marker		Morphometric analysis											Molecular biological analysis			
Wound age		Cell number						Ratios					Western blotting		qPCR	
		A	B	C	D	E	F	B/A	C/A	D/A	D/B	F/E	Pax7	MyoD	*Pax7*	*Myod1*
Time after injury (days)	1							>0.29		<0.25						
	3															>2.59
	5	>89	>6	>34		>39	>83						>1.13			
	5–7			>16		>20										
	3–7												>0.73	>1.33	>2.38	
	3–9	>60			>47		>58				>18.30					

A total satellite cells, *B* $Pax7^+/MyoD^-$ cells, *C* $Pax7^+/MyoD^+$ cells, *D* $Pax7^-/MyoD^+$ cells, *E* $Pax7^+$ cells, *F* $MyoD^+$ cells

muscle injury. Morphometrically, the $Pax7^+$ and $MyoD^+$ cells also increased in number in the similar pattern. We speculated that the upregulated Pax7 expression may be associated with the increased $Pax7^+$ cell number. Moreover, inflammatory response is essential for muscle regeneration, and the infiltrating inflammatory cells not only phagocytize cellular debris but also play roles in muscle regeneration by releasing a series of cytokines and growth factors [30], which may cause the peak of Pax7 and MyoD expressions in inflammatory stage of muscle injury.

In forensic practice, histopathological and immunohistochemical procedures were conventionally employed for wound age estimation by most researchers [12, 14, 17, 20, 31]. Therefore, we attempted to estimate the wound age by morphometrical analysis in this study. It suggests that the wound age may range from 3 to 9 days for the number of $Pax7^-/MyoD^+$ cells >47, the total number of satellite cells >60, the ratios of $Pax7^-/MyoD^+$ to $Pax7^+/MyoD^-$ cells >18.30, or the $MyoD^+$ cell number >58. For the number of $Pax7^+/MyoD^+$ cells >16 or $Pax7^+$ cells >20, it possibly indicates a wound age of 5 to 7 days. The ratios of $Pax7^+/MyoD^-$ cells to total satellite cell number >0.29 or the ratios of $Pax7^-/MyoD^+$ cells to total satellite cells <0.25 may be a parameter of 1 day post-injury, while the total number of satellite cells

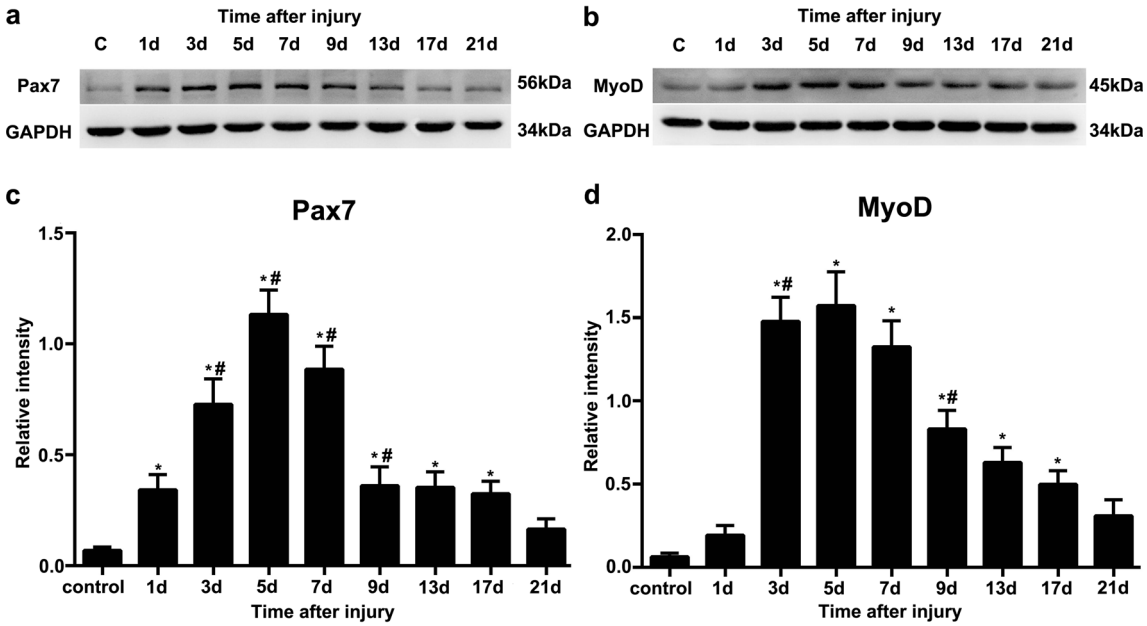

Fig. 5 **a** Analysis of Pax7 and GAPDH from skeletal muscle specimens by Western blotting. *Lane C* represents the result of the control skeletal muscle sample. Representative results from five individual animals are shown. **b** Analysis of MyoD and GAPDH from skeletal muscle specimens by Western blotting. *Lane C* represents the result of the control skeletal muscle sample. Representative results from five individual animals are shown. **c** Relative intensity of Pax7 to GAPDH. **d** Relative intensity of MyoD to GAPDH. All values are expressed as the mean±SD (n=5). *p<0.05 (vs control group), $^{\#}p$<0.05 (vs preceding posttraumatic group)

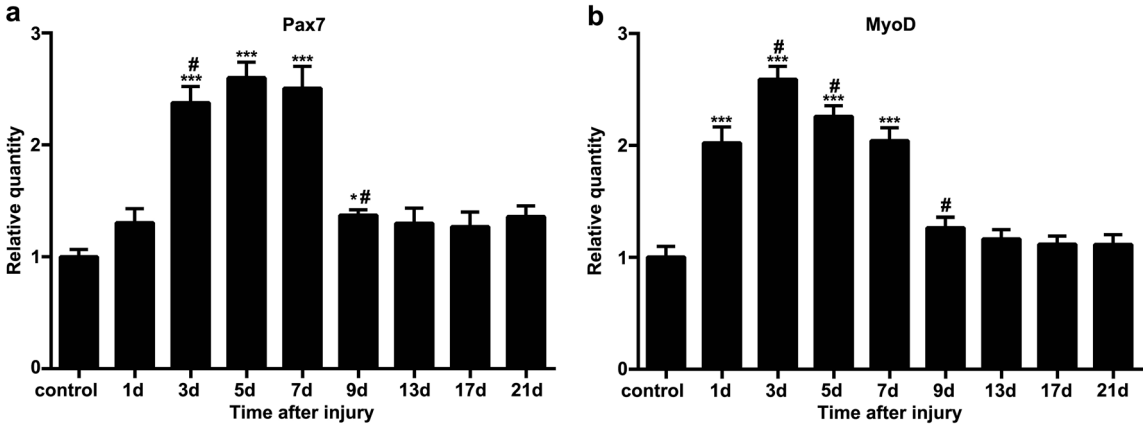

Fig. 6 **a** Relative quantity of Pax7 mRNA expression. All values are expressed as the mean±SD ($n=5$). *$p<0.05$ (vs control group); ***$p<0.001$ (vs control group); #$p<0.05$ (vs preceding posttraumatic group) **b** Relative quantity of MyoD mRNA expression. All values are expressed as the mean±SD ($n=5$). ***$p<0.001$ (vs control group); #$p<0.05$ (vs preceding posttraumatic group)

>89, the $Pax7^+/MyoD^-$ cell number >6, the $Pax7^+/MyoD^+$ cell number >34, the $Pax7^+$ cell number >39, or the $MyoD^+$ cell number >83 may indicate 5 days post-injury.

Recently, some markers for estimating wound age display regular expressions following injury [18]. Nevertheless, the quantitative data of the markers are always debatable in court. It is necessary to obtain comprehensive results by combining different methods [32]. Techniques of Western blotting and qPCR have been applied to wound age estimation, implying that the markers of wound age may be detected more accurately [23, 33]. In addition, mRNA is inducted before the protein synthesis [33–35], which makes mRNA a more appropriate parameter in early wound age estimation. Moreover, combined detection of protein and mRNA may be more stable and sensitive than morphometrical assays alone for judging wound age [23]. Therefore, we also attempted to use Western blotting and qPCR to investigate the expressions of Pax7 and MyoD and found that the data obtained from the two techniques confirmed the results of morphometrical analysis. In Western blotting results, the relative quantity of Pax7 peaked at 5 days after injury (>1.13), which suggests a wound age of 5 days. The relative quantity of Pax7 >0.73 or MyoD >1.33 suggests a wound age of 3 to 7 days. The pattern of Pax7 and MyoD mRNA expressions detected by qPCR was similar to that of Pax7 and MyoD protein expressions. The relative quantity of MyoD mRNA expression peaked at 3 days after injury, which was >2.59 suggests a wound age of 3 days. The relative quantity of Pax7 mRNA >2.38 suggests a wound age of 3 to 7 days post-injury. When comprehensively analyzed the data of morphology in combination with those of Western blotting and qPCR, we found that the ratios of $MyoD^+$ cells to $Pax7^+$ cells >4.76, the relative quantity of Pax7 protein >0.73, the relative quantity of MyoD protein >1.33, and the relative quantity of Pax7 mRNA >2.38 may estimate a wound age of 3 days post-injury, which provides more accurate parameters for wound age estimation by the conjoint analysis. However, for forensic practical application, it is essential to collect human skeletal muscle samples with a variety of wound ages and further examine the suitability of Pax7 and MyoD in autopsy cases by qPCR, Western blotting and morphometrical analysis.

In conclusion, expressions of Pax7 and MyoD were upregulated during skeletal muscle wound healing in rats. The time-dependent expressions of Pax7 and MyoD may provide new reference and more solid information for the wound age estimation in skeletal muscle contusion.

Acknowledgments The study was financially supported in part by grants from research fund for the Doctoral Program funded by Ministry of Education of China (20122104110025) and from projects funded by National Natural Science Foundation of China (81273342) and Shenyang Science and Technology Bureau (F12-277-1-03).

References

1. von Maltzahn J, Jones AE, Parks RJ, Rudnicki MA (2013) Pax7 is critical for the normal function of satellite cells in adult skeletal muscle. Proc Natl Acad Sci U S A 110:16474–16479
2. Ogura Y, Mishra V, Hindi SM, Kuang S, Kumar A (2013) Proinflammatory cytokine tumor necrosis factor (TNF)-like weak inducer of apoptosis (TWEAK) suppresses satellite cell self-renewal through inversely modulating notch and NF-κB signaling pathways. J Biol Chem 288:35159–35169
3. Figeac N, Serralbo O, Marcelle C, Zammit PS (2014) ErbB3 binding protein-1 (Ebp1) controls proliferation and myogenic differentiation of muscle stem cells. Dev Biol 386:135–151
4. Rahman MM, Ghosh M, Subramani J, Fong GH, Carlson ME, Shapiro LH (2014) CD13 regulates anchorage and differentiation of the skeletal muscle satellite stem cell population in ischemic injury. Stem Cells 32:1564–1577
5. Yin H, Price F, Rudnicki MA (2013) Satellite cells and the muscle stem cell niche. Physiol Rev 93:23–67
6. Relaix F, Zammit PS (2012) Satellite cells are essential for skeletal muscle regeneration: the cell on the edge returns centre stage. Development 139:2845–2856

7. Olguin HC, Olwin BB (2004) Pax-7 up-regulation inhibits myogenesis and cell cycle progression in satellite cells: a potential mechanism for self-renewal. Dev Biol 275:375–388
8. Motohashi N, Asakura A (2014) Muscle satellite cell heterogeneity and self-renewal. Front Cell Dev Biol 2:1
9. Olguin HC, Yang Z, Tapscott SJ, Olwin BB (2007) Reciprocal inhibition between Pax7 and muscle regulatory factors modulates myogenic cell fate determination. J Cell Biol 177:769–779
10. Diao Y, Guo X, Li Y, Sun K, Lu L, Jiang L, Fu X, Zhu H, Sun H, Wang H (2012) Pax3/7BP is a Pax7-and Pax3-binding protein that regulates the proliferation of muscle precursor cells by an epigenetic mechanism. Cell Stem Cell 11:231–241
11. Hayashi T, Ishida Y, Kimura A, Takayasu T, Eisenmenger W, Kondo T (2004) Forensic application of VEGF expression to skin wound age determination. Int J Legal Med 118:320–325
12. Ishida Y, Kimura A, Nosaka M, Kuninaka Y, Takayasu T, Eisenmenger W, Kondo T (2012) Immunohistochemical analysis on cyclooxygenase-2 for wound age determination. Int J Legal Med 126:435–440
13. Kondo T, Ishida Y (2010) Molecular pathology of wound healing. Forensic Sci Int 203:93–98
14. Kondo T, Tanaka J, Ishida Y, Mori R, Takayasu T, Ohshima T (2002) Ubiquitin expression in skin wounds and its application to forensic wound age determination. Int J Legal Med 116:267–272
15. Zheng JL, Yu TS, Li XN, Fan YY, Ma WX, Du Y, Zhao R, Guan DW (2012) Cannabinoid receptor type 2 is time-dependently expressed during skin wound healing in mice. Int J Legal Med 126:807–814
16. van de Goot FR, Korkmaz HI, Fronczek J, Witte BI, Visser R, Ulrich MM, Begieneman MP, Rozendaal L, Krijnen PA, Niessen HW (2014) A new method to determine wound age in early vital skin injuries: a probability scoring system using expression levels of fibronectin, CD62p and factor VIII in wound hemorrhage. Forensic Sci Int 244:128–135
17. Kondo T, Ohshima T, Mori R, Guan DW, Ohshima K, Eisenmenger W (2002) Immunohistochemical detection of chemokines in human skin wounds and its application to wound age determination. Int J Legal Med 116:87–91
18. Kondo T (2007) Timing of skin wounds. Leg Med (Tokyo) 9:109–114
19. Zhao R, Guan DW, Zhang W, Du Y, Xiong CY, Zhu BL, Zhang JJ (2009) Increased expressions and activations of apoptosis-related factors in cell signaling during incised skin wound healing in mice: a preliminary study for forensic wound age estimation. Leg Med (Tokyo) 11(Suppl 1):S155–S160
20. Ishida Y, Kimura A, Takayasu T, Eisenmenger W, Kondo T (2009) Detection of fibrocytes in human skin wounds and its application for wound age determination. Int J Legal Med 123:299–304
21. Yu TS, Cheng ZH, Li LQ, Zhao R, Fan YY, Du Y, Ma WX, Guan DW (2010) The cannabinoid receptor type 2 is time-dependently expressed during skeletal muscle wound healing in rats. Int J Legal Med 124:397–404
22. Sun JH, Wang YY, Zhang L, Gao CR, Zhang LZ, Guo Z (2010) Time-dependent expression of skeletal muscle troponin I mRNA in the contused skeletal muscle of rats: a possible marker for wound age estimation. Int J Legal Med 124:27–33
23. Fan YY, Zhang ST, Yu LS, Ye GH, Lin KZ, Wu SZ, Dong MW, Han JG, Feng XP, Li XB (2014) The time-dependent expression of α7nAChR during skeletal muscle wound healing in rats. Int J Legal Med 128:779–786
24. Zhang ST, Zhao R, Ma WX, Fan YY, Guan WZ, Wang J, Ren P, Zhong K, Yu TS, Pi JB, Guan DW (2013) Nrf1 is time-dependently expressed and distributed in the distinct cell types after trauma to skeletal muscles in rats. Histol Histopathol 28:725–735
25. Fan YY, Ye GH, Lin KZ, Yu LS, Wu SZ, Dong MW, Han JG, Feng XP, Li XB (2013) Time-dependent expression and distribution of Egr-1 during skeletal muscle wound healing in rats. J Mol Histol 44:75–81
26. Mokalled MH, Johnson AN, Creemers EE, Olson EN (2012) MASTR directs MyoD-dependent satellite cell differentiation during skeletal muscle regeneration. Genes Dev 26:190–202
27. Wang YX, Rudnicki MA (2011) Satellite cells, the engines of muscle repair. Nat Rev Mol Cell Biol 13:127–133
28. Hatade T, Takeuchi K, Fujita N, Arakawa T, Miki A (2014) Effect of heat stress soon after muscle injury on the expression of MyoD and myogenin during regeneration process. J Musculoskelet Neuronal Interact 14:325–333
29. Holterman CE, Rudnicki MA (2005) Molecular regulation of satellite cell function. Semin Cell Dev Biol 16:575–584
30. Prisk V, Huard J (2003) Muscle injuries and repair: the role of prostaglandins and inflammation. Histol Histopathol 18:1243–1256
31. Betz P (1994) Histological and enzyme histochemical parameters for the age estimation of human skin wounds. Int J Legal Med 107:60–68
32. Cecchi R (2010) Estimating wound age: looking into the future. Int J Legal Med 124:523–536
33. Ma WX, Yu TS, Fan YY, Zhang ST, Ren P, Wang SB, Zhao R, Pi JB, Guan DW (2011) Time-dependent expression and distribution of monoacylglycerol lipase during the skin-incised wound healing in mice. Int J Legal Med 125:549–558
34. Ohshima T, Sato Y (1998) Time-dependent expression of interleukin-10 (IL-10) mRNA during the early phase of skin wound healing as a possible indicator of wound vitality. Int J Legal Med 111:251–255
35. Bai R, Wan L, Shi M (2008) The time-dependent expressions of IL-1beta, COX-2, MCP-1 mRNA in skin wounds of rabbits. Forensic Sci Int 175:193–197